Supporting Information

Structural Basis of Polyketide Synthase *O*-Methylation

Meredith A. Skiba[a,b ○,▽], Marissa M. Bivins[a,○,Δ], John R. Schultz[d], Steffen M. Bernard[a,c,#], William D. Fiers[d,§], Qingyun Dan[a], Sarang Kulkarni[e], Peter Wipf[e], William H. Gerwick[f,g], David H. Sherman[a,h,i,j], Courtney C. Aldrich[d], Janet L. Smith[a,b*]

[a]Life Sciences Institute, University of Michigan, Ann Arbor, MI, 48109, United States
[b]Department of Biological Chemistry, University of Michigan, Ann Arbor, MI, 48109, United States
[c]Chemical Biology Doctoral Program, University of Michigan, Ann Arbor, MI, 48109, United States
[d]Department of Medicinal Chemistry, University of Minnesota, Minneapolis, MN, 55455, United States
[e]Department of Chemistry, University of Pittsburgh, Pittsburgh, PA, 15206, United States
[f]Center for Marine Biotechnology and Biomedicine, Scripps Institution of Oceanography, University of California San Diego, La Jolla, CA, 92093, United States
[g]Skaggs School of Pharmacy and Pharmaceutical Sciences, University of California San Diego, La Jolla, CA, 92093, United States
[h]Department of Medicinal Chemistry, University of Michigan, Ann Arbor, MI, 48109, United States
[i]Department of Chemistry, University of Michigan, Ann Arbor, MI, 48109, United States
[j]Department of Microbiology and Immunology, University of Michigan, Ann Arbor, MI, 48109, United States

°These authors contributed equally to this work
*To whom correspondence should be addressed JanetSmith@umich.edu

Present Addresses
▽ Department of Biological Chemistry and Molecular Pharmacology, Harvard Medical School, Boston, MA 02115, United States
Δ Department of Pharmacology, University of North Carolina at Chapel Hill, Chapel Hill, NC, 27599, United States
Department of Integrative Structural and Computational Biology, The Scripps Research Institute, La Jolla, CA, 92037, United States
§ Gastroenterology and Hepatology Division, Joan and Sanford I. Weill Department of Medicine, Weill Cornell Medicine, New York, NY, 10021, United States
The Jill Roberts Institute for Research in Inflammatory Bowel Diseases, Weill Cornell Medicine, New York, NY, 10021, United States

Construct Design

StiD and StiE constructs were amplified from codon optimized DNA (IDT) encoding regions of *stiD* (CAD19088.1) and s*tiE* (CAD19089.1) from *Stigmatella aurantiaca Sg a15*.[1] CurL constructs were amplified from a cosmid library.[2] Constructs encoding StiD *O*-MT (residues 956-1266, pMAS162; residues 976-1266, pMAS165), StiD ACP (residues 1794-1929, pMAS201), StiE *O*-MT (residues 942-1257, pMAS198), StiE ACP (residues 1789-1927, pMAS283), and CurL *O*-MT (residues 981-1315, pMAS411) were inserted into pMCSG7[3] and a construct encoding CurL *O*-MT (residues 951-1315, pMAS/SMB134) was inserted into pMOCR[4] by ligation independent cloning. *stiE* mutations were introduced into pMAS198 (E1102A, pMAS432; Y954F, pMAS433; E1102Q, pMAS434; L1106H, pMAS435; Y1209F, pMAS437; Y1223F, pMAS439), *curL* mutations were introduced into pMAS/SMB134 (Y1010F, pMAS416; E1161A, pMAS428; E1161Q, pMAS430; H1165A, pMAS413; H1165N, pMAS412; Y1267F, pMAS408; Y1281F, pMAS429) using the QuickChange protocol (Stratagene). All constructs and mutations were verified by Sanger sequencing at the University of Michigan DNA Sequencing Core.

Protein Expression and Purification

Plasmids containing *O*-MTs and ACPs were transformed into *Escherichia coli* strain BL21(DE3). Transformed cells were grown in 0.5 L of TB media at 37°C supplemented with 100 μg mL^{-1} ampicillin to an OD_{600}=1-2, cooled to 20°C for 1 hr, and induced with 200 μM isopropyl β-D-1-thiogalactopyranoside (IPTG) for 18 hrs. Media to produce StiD, StiE, and CurL ACP was supplemented with a trace metal mix to insure production of apo-ACP, lacking the phosphopantetheine post translational modification.[5] Selenomethionine (SeMet) labeled StiD *O*-MT (residues 976-1266) was produced in 2L of SelenoMet medium (AthenaES) containing 150 μg/mL seleno-DL-methionine. Cultures were grown to an OD_{600}=0.6 at 37°C, cooled to 20°C for 1 hr, and induced with 200 μM IPTG for 18 hrs.[6]

Cell pellets were resuspended in 35 mL Tris buffer A (50 mM Tris pH 7.4, 300 mM NaCl, 10% glycerol, 20 mM imidazole) with 0.1 mg mL^{-1} lysozyme, 0.05 mg mL^{-1} DNase, and 2 mM $MgCl_2$, incubated on ice for 30 min, lysed by sonication, and cleared by centrifugation (38,760 x g, 30 min, 4°C). The supernatant was filtered and loaded onto a 5 mL His trap column (GE Healthcare). Proteins were eluted with a 5-100% linear gradient of Tris buffer B (50 mM Tris 7.4, 300 mM NaCl, 10% glycerol, 400 mM imidazole) over 10 column volumes. The His-Tag and/or Mocr

fusion was removed from StiD *O*-MT (residues 956-1266), StiE *O*-MT (residues 942-1257), CurL *O*-MT (residues 981-1315 and 951-1315), StiE ACP, and CurL ACP via incubation with tobacco etch virus (TEV) protease. The cleavage reaction mixture was dialyzed overnight into Tris buffer A to remove imidazole. Protein lacking the His-tag was isolated by passing over a second His trap column. Proteins were further purified by gel filtration (*O*-MTs, HiLoad 16/60 Superdex S200; ACPs, HiLoad 16/60 Superdex S75) in Tris buffer C (50 mM Tris pH 7.4, 150 mM NaCl, 10% glycerol). Apparent molecular weights were determined by analytical size exclusion chromatography (10/300 Superdex S200 Increase equilibrated with Tris Buffer C).

In order to produce holo StiD ACP, 113 μM StiD ACP was incubated with 0.5 mM coenzyme A (CoA) and 20 μM *Streptomyces verticillus* phosphopantetheinyl transferase (SVP)[7] in Tris buffer C with 20 mM $MgCl_2$ and 2 mM DTT at 20 °C overnight to produce holo-ACP. The His-tag was simultaneously removed by the addition of 12 μM TEV protease. Holo-ACP lacking the His-tag was purified from the reaction mixture by passing over a 1 mL His trap column. Purified holo-ACP was dialyzed into Tris buffer C. StiD ACP concentration was determined using the DC protein assay (BioRad).

General Chemistry Procedures

All chemical reagents were used as provided unless indicated otherwise. Tetrahydrofuran (THF) and dichloromethane (CH_2Cl_2) were purified via passage through neutral alumina columns. Ethyl acetate was purified by drying over 4 Å molecular sieves. Compounds were purified by flash chromatography using silica gel (300–400 mesh) in the indicated solvent system. TLC was performed using 250 μm, F254 silica gel plates and visualized by UV or through staining with para-anisaldehyde or potassium permanganate. Optical rotations were acquired on a polarimeter at the indicated temperature using the sodium D line (λ = 589 nm) unless otherwise specified and reported as follows: [α] λ Temp = rotation (c g/100 mL, solvent). ^{1}H and ^{13}C NMR spectra were recorded on a 500 MHz NMR spectrometer. Chemical shifts are reported in ppm based on an internal standard of residual $CHCl_3$ (7.26 ppm in ^{1}H NMR and 77.16 in ^{13}C NMR). Proton chemical data are reported in the following format: chemical shift (ppm), multiplicity (s = singlet, d = doublet, t = triplet, q = quartet, quint = quintet, sext = sextet, sept = septet, m = multiplet, br = broad peak, app = apparent), coupling constant(s), and integration. High-resolution mass spectra

(HRMS) were obtained on a time-of-flight (TOF) mass spectrometer using either PEG or PPG standards to calibrate the instrument.

Scheme 1. Synthesis of *N*-acetylcysteamine (NAC)-linked triketide substrates

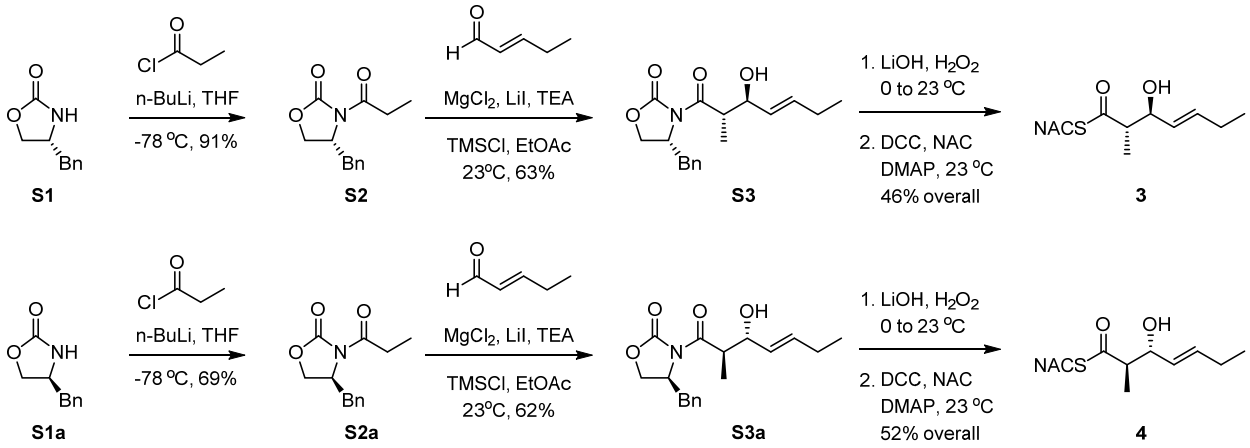

The synthesis of the two *anti*-enantiomers of the *N*-acetylcysteamine (NAC) linked triketide substrates **3** and **4** began with acylation of L-phenylalanine and D-phenylalanine-derived oxazolidinone chiral auxiliaries with propionyl chloride.[8] The non-Evans *anti*-aldol products (**S2** and **S2a**) were obtained in much better yields than previously reported [9] by utilization of a modified magnesium halide-catalyzed anti-aldol reaction. [10] The final NAC liked triketide substrates were prepared by removal of the oxaozolidinone auxiliary via lithium hydroperoxide followed by DCC-mediated coupling of NAC in the presence of catalytic DMAP. The other two *syn*-diastereomers, compounds **S1** and **S1a**, were synthesized as previously reported.[10]

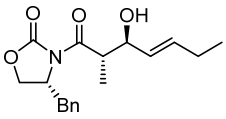

(4*S*)-4-Benzyl-3-[(2*S*,3*S*,4*E*)-3-hydroxy-2-methylhept-4-enoyl)]oxazolidinone (S3). To a flame-dried reaction vessel under an argon atmosphere equipped with a stir bar, oxazolidinone **S2** (0.100 g, 0.429 mmol), $MgCl_2$ (0.038 g, 0.40 mmol), LiI (0.106 g, 0.79 mmol), EtOAc (0.85 mL), Et_3N (0.27 mL, 1.89 mmol) and TMSCl (0.20 mL, 1.50 mmol) were added sequentially. After 10 min of stirring trans-2-penten-1-al (0.585 mL, 1.17 mmol, 2M in EtOAc) was slowly added over 3 h at 23 °C. The reaction mixture was monitored by TLC and was complete at 5 h. The reaction mixture was passed through a plug of silica gel using EtOAc as the eluent.

After removing the solvent in vacuo, MeOH (4 mL) and *p*-TsOH (25 mg) were added. After 45 min desilylation was complete as judged by TLC. The crude reaction was concentrated onto silica gel and purified by flash column chromatography (9:1 to 7:3 Hexanes-EtOAc stepwise gradient) to give the title compound (0.084 g, 63%) as a viscous, colorless oil: R_f = 0.25 (7:3 hexanes−EtOAc); $[\alpha]_D^{24}$ = −27.6 (*c* 1.00, $CHCl_3$); ^{1}H NMR ($CDCl_3$, 500 MHz) δ 7.29 (m, 5H), 5.81 (dt, *J* = 15.3, 6.3 Hz, 1H), 5.51 (dd, *J* = 15.4, 7.3 Hz, 1H), 4.70 (m, 1H), 4.18 (m, 3H), 3.95 (m, 1H), 3.29 (dd, *J* = 13.5, 2.9 Hz, 1H), 2.78 (dd, *J* = 13.5, 9.4 Hz, 1H), 2.57 (m, 1H), 2.09 (q, *J* = 7.4 Hz, 2H), 1.17 (d, *J* = 6.9 Hz, 3H), 1.01 (t, *J* = 7.5 Hz, 3H); ^{13}C NMR ($CDCl_3$, 500 MHz) δ 206.7, 176.5, 153.5, 135.9, 135.3, 129.5, 129.2, 128.9, 127.3, 75.8, 66.0, 55.5, 43.4, 37.8, 30.9, 25.2, 14.5, 13.4.

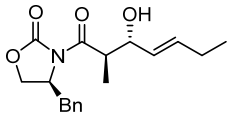

(4*R*)-4-Benzyl-3-[(2*R*,3*R*,4*E*)-3-hydroxy-2-methylhept-4-enoyl)]oxazolidinone (S3a). To a flame-dried reaction vessel under an argon atmosphere equipped with a stir bar, oxazolidinone **S2a** (0.200 g, 0.857mmol), $MgCl_2$ (0.082 g, 0.86 mmol), LiI (0.225 g, 0.1.68 mmol), EtOAc (1.60 mL), Et_3N (0.57 mL, 4.04 mmol) and TMSCl (0.42 mL, 3.22 mmol) were added sequentially. After 10 min of stirring *trans*-2-pentene-1-al (1.25 mL, 2.49 mmol, 2M in EtOAc) was slowly added over 3 h at 23 °C. The reaction mixture was monitored by TLC and was finished at 5 h. The reaction mixture was passed through a plug of silica gel using EtOAc as the eluent. After removing the solvent in vacuo, MeOH (4 mL) and p-TsOH (25 mg) were added. After 45 min desilylation was complete as judged by TLC. The crude reaction was concentrated onto silica gel and purified by flash column chromatography (9:1 to 7:3 Hexanes-EtOAc stepwise gradient) to give 7 (0.168 g, 62%) as a viscous, yellow oil: Rf = 0.25 (7:3 hexanes−EtOAc); $[\alpha]_D^{24}$ = 27.1 (*c* 1.00, $CHCl_3$); ^{1}H NMR ($CDCl_3$, 500 MHz) δ 7.29 (m, 5H), 5.81 (dt, *J* = 15.9, 6.1 Hz, 1H), 5.52 (dd, *J* = 15.4, 7.2 Hz, 1H), 4.70 (m, 1H), 4.17 (m, 3H), 3.95 (m, 1H), 3.30 (dd, *J* = 13.6, 3.3 Hz, 1H), 2.78 (dd, *J* = 13.6, 9.4 Hz, 1H), 2.57 (m, 1H), 2.09 (q, *J* = 7.3 Hz, 2H), 1.18 (d, *J* = 7.3 Hz, 3H), 1.01 (t, *J* = 7.4 Hz, 3H); ^{13}C NMR ($CDCl_3$, 500 MHz) δ 206.7, 176.5, 153.5, 135.9, 135.3, 129.5, 129.2, 128.9, 127.3, 75.8, 66.0, 55.5, 43.4, 37.8, 30.9, 25.2, 14.5, 13.4.

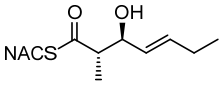

S-(2-Acetamidoethyl) (2*S*,3*S*,4*E*)-3-hydroxy-2-methylhept-4- enethioate (3). To a stirring solution of **S3** (56 mg, 0.169 mmol) in THF (0.6 mL) at 0 °C was added aqueous H_2O_2 (30% *v/v*, 0.245 mL) dropwise. Aqueous LiOH (1.19 mL, 0.4 M) was then added portionwise to the stirring solution and the reaction was allowed to warm to room temperature and stirred for 5 h. The reaction was quenched by the addition of Na_2SO_3 (5 mL) then concentrated under reduced pressure. The crude material was portioned between CH_2Cl_2 (10 mL) and 10% NaOH (5 mL) and the organic layer was discarded. The aqueous layer was then acidified to a pH of 1 with 1 M HCl and extracted with CH_2Cl_2 (3 × 10 mL). The organics were dried over $MgSO_4$, filtered, and then concentrated to afford the crude acid. To a solution of the crude acid (28 mg, 0.168 mmol) in CH_2Cl_2 (1.69 mL) added *N*-acetylcysteamine (80 mg, 0.67 mmol), *N*,*N*'-dicyclohexylcarbodiimide (45 mg, 0.22 mmol), and 4-(dimethylamino)pyridine (1 mg, 0.009 mmol) sequentially. The reaction was stirred vigorously for 26 h. The reaction was filtered, concentrated and directly purified by flash chromatography (85:15:5 toluene-CH_2Cl_2–MeOH) to afford the title compound (20 mg, 46% over 2 steps) as a light yellow, viscous oil: R_f = 0.30 (95:5 CH_2Cl_2–MeOH); $[\alpha]_D^{24}$ = 37.1 (*c* 0.35, $CHCl_3$); ^{1}H NMR ($CDCl_3$, 400 MHz) δ 5.88 (br s, 1H), 5.79 (dt, *J* = 15.6, 6.0 Hz, 1H), 5.40 (ddt, *J* = 15.6, 6.4, 1.2 Hz, 1H), 4.21 (t, *J* = 7.6 Hz, 1H), 3.55–3.37 (m, 2H), 3.13–2.98 (m, 2H), 2.76 (quint, *J* = 7.2 Hz, 1H), 2.07 (app. quint, *J* = 7.6 Hz, 2H), 1.96 (s, 3H), 1.13 (d, *J* = 6.8 Hz, 3H), 1.00 (t, *J* = 7.6 Hz, 3H); ^{13}C NMR ($CDCl_3$, 100 MHz) δ 203.7, 170.6, 136.8, 128.8, 75.6, 54.5, 39.7, 28.7, 25.4, 23.3, 15.2, 13.5; HRMS (ESI+) *m/z* calcd for $C_{12}H_{21}NO_3SNa^+$ [M + Na]+ 282.1134, found 282.1158 (error 8.5 ppm).

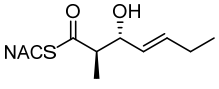

S-(2-Acetamidoethyl) (2*R*,3*R*,4*E*)-3-hydroxy-2-methylhept-4-enethioate (4). The thioester **4** was synthesized in an analogous manner to that of the enantiomer **S3** furnishing the desired product (23 mg, 52%) as a light yellow, viscous oil: R_f = 0.30 (95:5 CH_2Cl_2–MeOH); $[\alpha]_D^{24}$ = −34.5 (*c* 0.29, $CHCl_3$); ^{1}H NMR ($CDCl_3$, 400 MHz) δ 6.00 (br s, 1H), 5.76 (dt, *J* = 15.6, 6.0 Hz, 1H), 5.40 (ddt, *J* = 15.6, 6.4, 1.2 Hz, 1H), 4.19 (t, *J* = 7.6 Hz, 1H), 3.55–3.37 (m, 2H), 3.13–2.98 (m, 2H), 2.76 (app. quint, *J* = 7.2 Hz, 1H), 2.42 (br s, 1H), 2.06 (app. quint, *J* = 7.6 Hz, 2H), 1.94 (s, 3H), 1.11 (d, *J* = 6.8 Hz, 3H), 1.00 (t, *J* = 7.6 Hz, 3H); ^{13}C NMR ($CDCl_3$, 100 MHz)

δ 203.6, 170.6, 136.6, 128.8, 75.5, 54.5, 39.5, 28.7, 25.4, 23.3, 15.1, 13.5; HRMS (ESI+) *m*/*z* calcd for $C_{12}H_{21}NO_3SNa^+$ $[M + Na]^+$ 282.1134, found 282.1151 (error 6.0 ppm).

Production of acyl-ACPs

N-acetylcysteamine (NAC)-linked diastereomeric triketide substrates (**1**, **2**) were synthesized as previously reported[9]. Holo StiD-ACP (50 μM) was incubated with 5 mM **1**, **2**, **3**, or **4** in 300 mM sodium bicarbonate pH 8.1 at 25°C for 4 hrs. ACP was buffer exchanged into reaction buffer (50 mM HEPES 7.4, 150 mM NaCl) and flash frozen.

(3*R*)-3-Hydroxy-5-methoxy-myristoyl-CoA was synthesized as previously reported[11]. Apo StiE-ACP (180 μM) was incubated with 36 μM SVP, 0.72 mM (3*R*)-3-hydroxy-5-methoxy-myristoyl-CoA, 20 mM $MgCl_2$ for 1 hr at 25°C in Tris C. The reaction mixture was passed over a 1 mL His Trap column (GE Healthcare) to isolate the ACP. StiE (3*R*)-3-hydroxy-5-methoxy-myristoyl-ACP was further purified via size exclusion chromatography (HiLoad 16/60 Superdex S75) equilibrated with Tris buffer C.

(*R*)-3-Hydroxydodecanoyl-CoA was synthesized as previously reported[12]. Apo CurL ACP (180 μM) was incubated with 20 μM SVP, 0.5 mM (*R*)-3-hydroxydodecanoyl-CoA, and 20 mM $MgCl_2$ for 4 hrs at 25°C in Tris buffer C. The reaction mixture was passed over a 1 mL His Trap column (GE Healthcare) to isolate the ACP. CurL (*R*)-3-hydroxydodecanoyl-ACP was further purified via size exclusion chromatography (HiLoad 16/60 Superdex S75) equilibrated with Tris buffer C.

Enzyme Assays

StiD triketide-ACP (**1**, **2**, **3**, **4**) (50 μM) was incubated with 25 μM StiD *O*-MT (956-1266) and 0.5 mM SAM in 50 mM HEPES pH 7.4, 150 mM NaCl, 0.5 mM $MgCl_2$. Reaction mixtures (10 μL) were incubated for 24 hrs at 25°C and quenched with 1% formic acid. 0.5 uL of reaction mixtures were subjected to LC/MS analysis.

StiE (3*R*)-3-hydroxy-5-methoxy-myristoyl-ACP (**6**) (50 μM) was incubated with 12.5 μM StiE *O*-MT (942-1257) variants or StiE *O*-MT (961-1257) and 0.5 mM SAM in 50 mM HEPES pH 7.4, 150 mM NaCl, 0.5 mM $MgCl_2$. Reaction mixtures (10 μL) were incubated for 15 minutes at 25°C and quenched with 1% formic acid. 1 uL of reaction mixtures were subjected to LC/MS analysis.

CurL (*R*)-3-hydroxydodecanoyl-ACP (**7**) (50 μM) was incubated with 12.5 μM CurL *O*-MT (951-1315) variants and 0.5 mM SAM in 50 mM HEPES pH 7.4, 150 mM NaCl, 0.5 mM $MgCl_2$. Reaction mixtures (10 μL) were incubated for 6 hrs at 25°C and quenched with 1% formic acid. 1 uL of reaction mixtures were subjected to LC/MS analysis.

Apo StiD, StiE, or CurL ACP (50 μM) were incubated with 10 uM SVP, 200 μM acetoacetyl-CoA, 0.5 mM SAM and StiD *O*-MT (951-1315), StiE *O*-MT (942-1257), or CurL *O*-MT (951-1315) variants in 50 mM HEPES pH 7.4, 150 mM NaCl, 0.5 mM $MgCl_2$. Reaction mixtures were incubated for 24 hrs at 25°C and quenched with 1% formic acid. 1 uL of reaction mixtures were subjected to LC/MS analysis.

Reaction mixtures were analyzed using the phosphopantetheine (Ppant) ejection method[13, 14] on an Agilent Q-TOF 6545. Samples were separated by reverse phase HPLC (Phenomenex Aeris widepore C4 column 3.6 μM, 50 x 2.10 mm) at a flow rate of 0.5 mL min^{-1} in H_2O with 0.2% (v/v) formic acid. Protein was eluted with a gradient of 5-100% acetonitrile with 0.2% (v/v) formic acid over 4 min. Data were processed using MassHunter Qualitative Analysis software (Agilent). Substrates and products in the StiD *O*-MT reactions experienced in-source decay yielding a conjugated dehydrated species.

Protein Crystallization and Structure Determination

SeMet labeled StiD *O*-MT (residues 976-1266 with His-tag) was crystallized at 4°C by sitting drop vapor diffusion from 2:2 μL mixture of protein stock (10 mg mL^{-1} StiD *O*-MT 976-1266 in Tris buffer C with 1 mM SAM) and well solution (27% PEG 4000, 0.77 M LiCl, 0.1 M Tris pH 7.0). Microseeding was used to obtain single diamond shaped crystals, which grew after 8 days. Crystals were harvested directly from the drop and flash cooled in liquid N_2.

Native StiD *O*-MT (residues 976-1266 with His-tag) was crystallized at 20°C by sitting drop vapor diffusion from 1:1 μL mixture of protein stock (11 mg mL^{-1} StiD *O*-MT 976-1266 in Tris buffer C with 1 mM SAM) and well solution (20% PEG 3350, 0.2 M NaF). Diamond shaped crystals grew after one week and were harvested directly from the drop and flash cooled in liquid N_2.

StiD *O*-MT (residues 956-1266, His-tag removed) was crystallized at 20°C by sitting drop vapor diffusion from a 2:1 μL mixture of protein stock (13 mg mL^{-1} StiD *O*-MT 956-1266 in Tris buffer C with 1 mM SAM) and well solution (1.5 M ammonium citrate tribasic pH 7.2). Microseeding

was used to obtain single rod-shaped crystals, which grew overnight. Crystals were cryoprotected with well solution supplemented with 20% glycerol and flash cooled in liquid N_2.

StiE *O*-MT (961-1257 with His-tag), was crystallized at 4°C by sitting drop vapor diffusion from 2:1 μL protein stock (11 mg/mL His-tagged StiE *O*-MT in Buffer C with 1 mM SAM or SAH) to well solution (10% PEG 3350, 0.1 M sodium formate). Microseeding was used to obtain single crystals. Square bipyramidal crystals grew in 3 days. Crystals were harvested directly from the drop and flash cooled in liquid nitrogen.

StiE *O*-MT (residues 942-1257, His-tag removed) was crystallized at 4°C by sitting drop vapor diffusion from a 2:1 μL protein stock (9 mg mL^{-1} StiE *O*-MT 961-1257 in Tris buffer C with 1 mM SAM) and well solution (25% PEG 8000, 0.1 M HEPES pH 7.4) at 4°C. Square bipyramidal crystals grew after 5 days. Crystals were cryoprotected in well solution supplemented with 20% glycerol and flash cooled in liquid N_2.

Diffraction data for all structures were collected at APS beamline 23ID-D or ID-B and processed using XDS.[15] The SeMet StiD *O*-MT 976-1266 was solved by single-wavelength anomalous diffraction (SAD) phasing using Phenix AutoSol[16] in the Phenix Software suite.[17] A nearly complete model was build using Phenix AutoBuild.[18] Native StiD *O*-MT 976-1266 was isomorphous with the SeMet crystal form. StiD *O*-MT 956-1266 and StiE *O*-MT 942-1257 were solved by molecular replacement using Phaser[19]. Iterative rounds of model building and refinement were carried out using Coot[20] and Phenix.refine[21] with automated translation/liberation/screw group selection. Structures were validated using MolProbity.[22] Homologs in the structure database were identified using the DALI server.[23] Sequence alignments were prepared using Clustal[24] through Jalview[25] and figures were prepared with PyMol.[26]

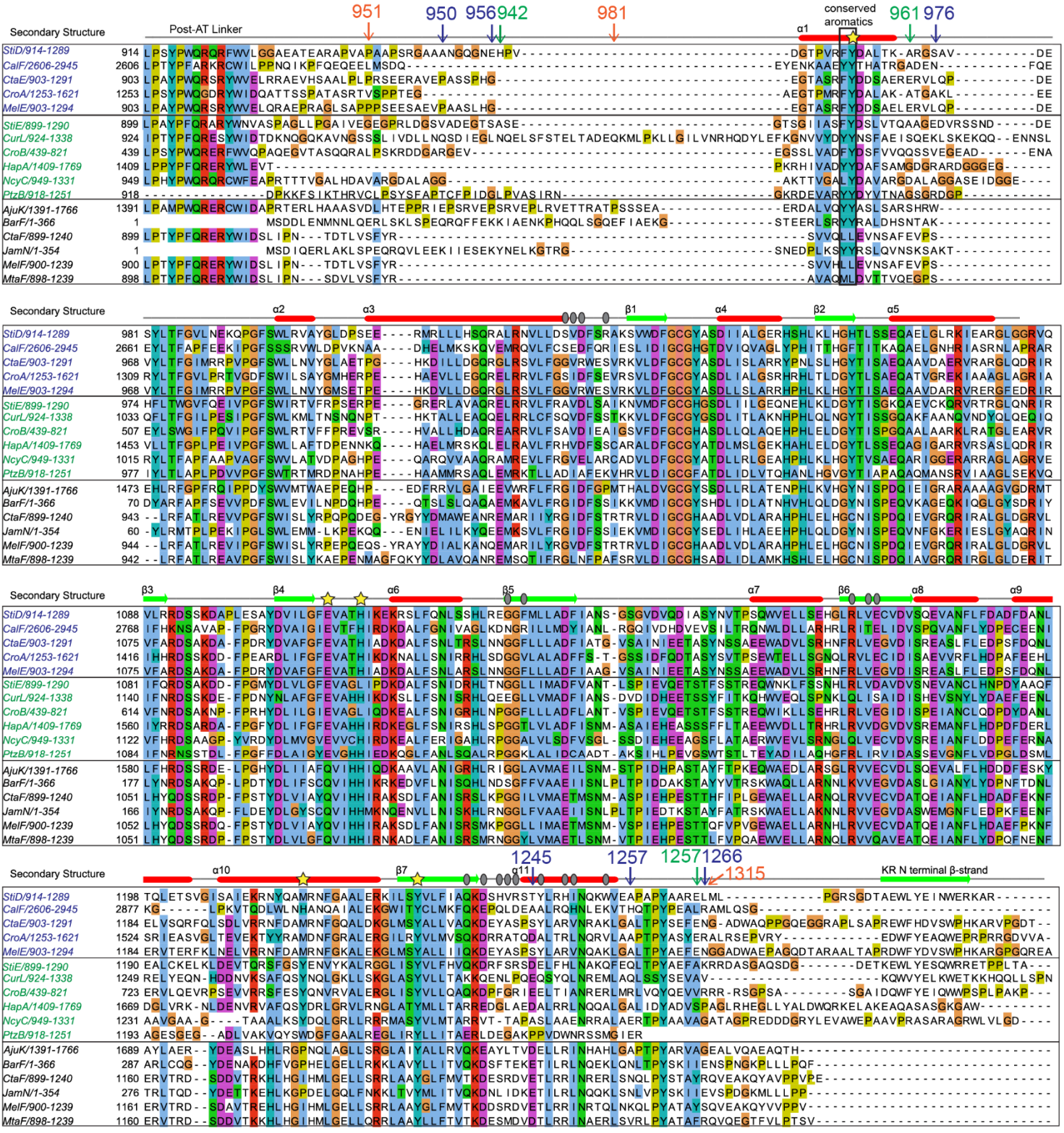

Figure S1. Sequence alignment of PKS *O*-MTs. Names are colored based on predicted substrate ((*S*)-OH, blue; (*R*)-OH, green; keto; black). Substrate predictions are based upon structures of the final metabolites, the inclusion of a KR in *O*-MT containing modules, and KR sequence motifs that correlate with the stereochemical configuration of the resulting methoxy. Stars indicate sites

of mutagenesis; arrows represent experimental N- and C-termini tested for StiD (blue) and fragment N- and C-termini for StiE (green) and CurL (orange). Gray ovals represent residues in the StiD or StiE *O*-MT dimer interface. Pathway abbreviations (GenBank Accision codes, *trans*/*cis*-AT, producing organism) are as follows: Sti- stigmatellin (CAD19088.1, CAD19089.1, *cis*-AT, *Stigmatella aurantiaca*); Cal- calyculin A (BAP05594.1, *trans*-AT, *Candidatus entotheonella* sp. A); Cta- cystothiazole A (AAW03329.1, AAW03329.1, *cis*-AT, *Cystobacter fuscus*); Cro- crocacin (AIR74910, AIR74911.1, *cis*-AT, *Chondromyces crocatus*); Mel- melithiazol (CAD89776.1, CAD89777.1, *cis*-AT, *Melittangium lichenicola*); Cur- curacin A (AEE88278.1, *cis*-AT, *Moorea producens*); Hap- haprolid (AOG74798.1, *cis*-AT, *Byssovorax cruenta*); Nyc- nannocystin A (ALD82523.1, *cis*-AT, *Nannocystis sp. MB1016*); Ptz- patellazole (AFX99666.1, *trans*-AT, *Candidatus Endolissoclinum faulkneri L2*); Aju- ajudazol (CAQ18838.1, *cis*-AT, *Chondromyces crocatus*); Bar- barbamide (AAN32980.1, *cis*-AT, *Lyngbya majuscula*); Jam- jamaicamide (AAS98785.1, *cis*-AT, *Lyngbya majuscula*); Mta- myxothiazol (AAF19814.1, *cis*-AT, *Stigmatella aurantiaca*).

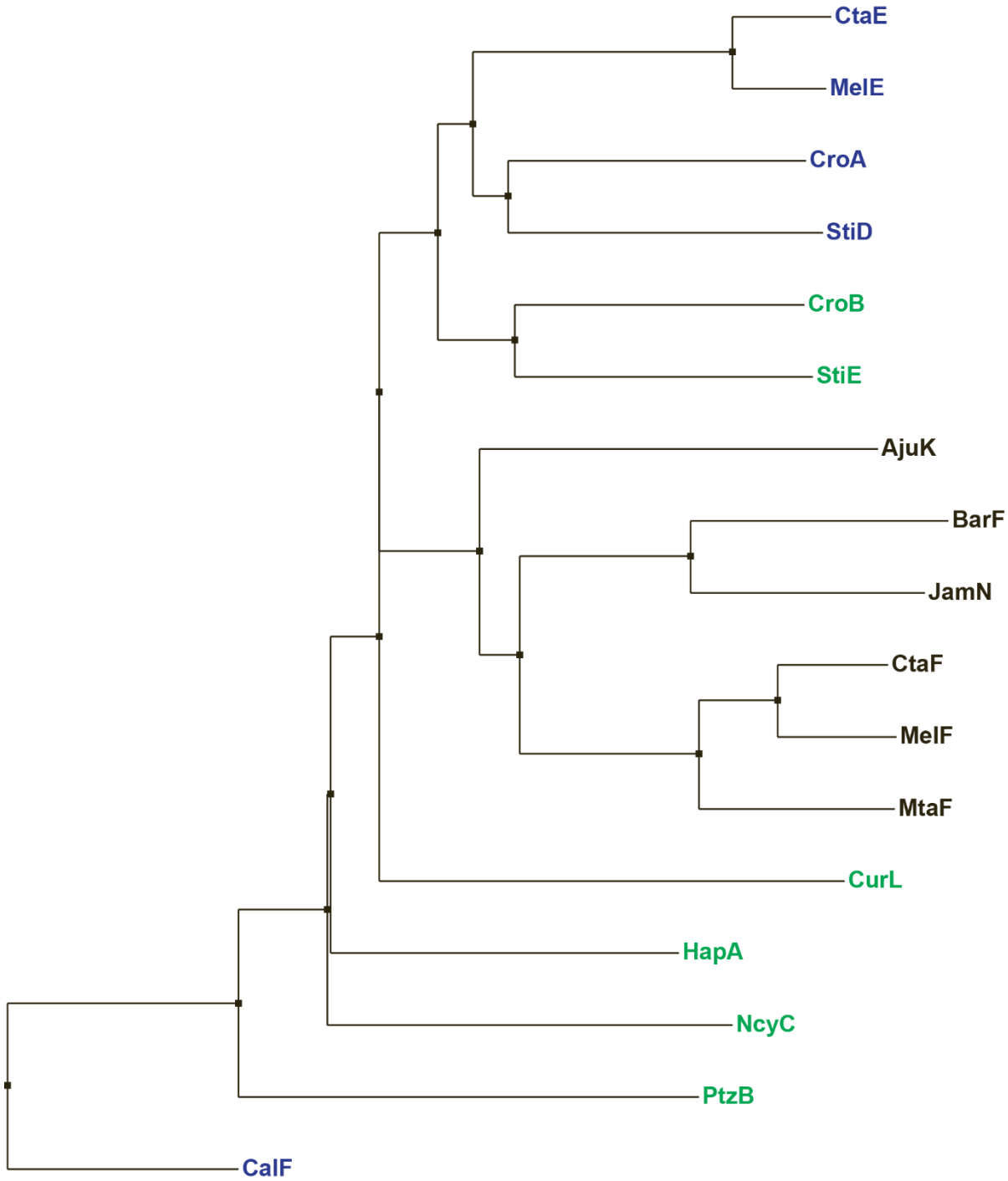

Figure S2. Dendrogram of PKS *O*-MTs from Figure S1. Names are colored based on predicted substrate ((*S*)-OH, blue; (*R*)-OH, green; keto, black) as in Figure S1. All *O*-MTs are from *cis*-AT PKS pathways except PtzB and CalF, which are from *trans*-AT pathways.

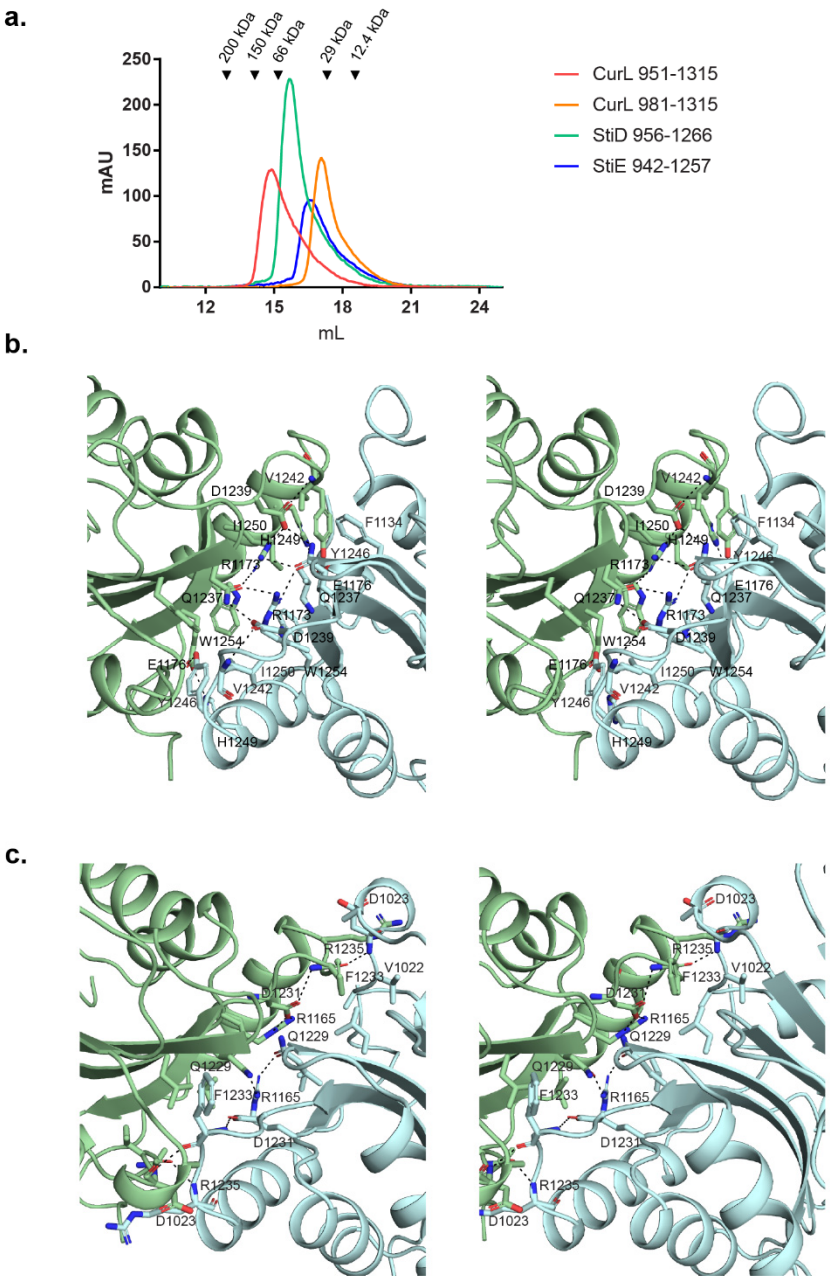

Figure S3. Oligomer state of *O*-MTs. **(a)** Size exclusion chromatography of *O*-MT fragments. StiD *O*-MT (amino acids 956-1266, 35 kDa monomer) elutes with an apparent molcular weight of 55 kDa and StiE *O*-MT (amino acids 942-1257, 37 kDa monomer) elutes predominantly as a monomer (apparent molecular weight 35.7 kDa). CurL *O*-MT (amino acids 981-1315, 39 kDa monomer) is exlusively monomeric (apparent molecular weight 26.9 kDa). Inclusion of a 30 residue post-AT dimerization element at the CurL N-terminus (amino acids 951-1315, 42 kDa monomer) results in dimeric protein (apparent molecular weight 82.8 kDa). **(b)** The StiD *O*-MT dimer interface is mediated by amino acids Phe1134, Arg1173, Val1175, Glu1176, Gln1237, Asp1239, Val1242, Tyr1246, His1249, Ile1250, Trp1254 from each monomer. **(c)** StiE *O*-MT dimer interface is mediated by amino acids Ala1021, Asp1023, Ala1026, Gly1124, Leu1126, Arg1165, Val1167, Gln1229, Asp1231, Phe1233, Arg1235.

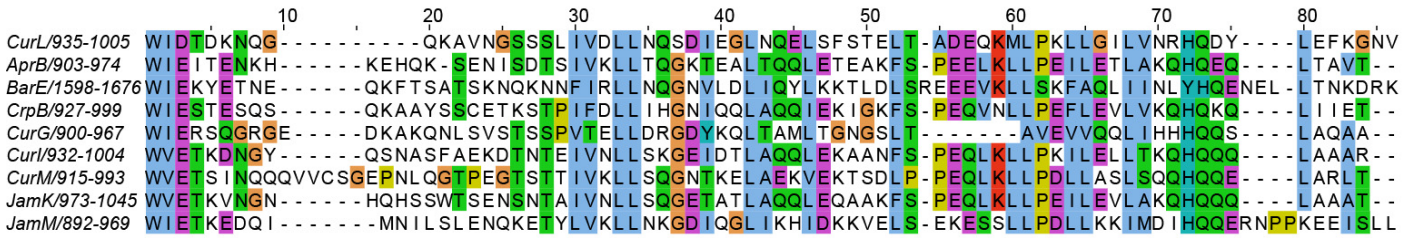

Figure S4. Sequence alignment of cyanobacterial post-AT dimerization elements. Pathway abbreviations (GenBank accesion codes) are as follows: Cur-curacin A (CurL, AEE88278.1; CurG, AEE88283.1; CurI, AEE88281.1; CurM, AAT70108.1), Apr- apratoxin A (AprB, WP_075900458), Bar- barbamide (BarE, AEE88299), Crp- cryptophycin (CrpB, ABM21570.1), Jam- jamaicamide (JamK, AAS98782.1; JamM, AAS98784.1).

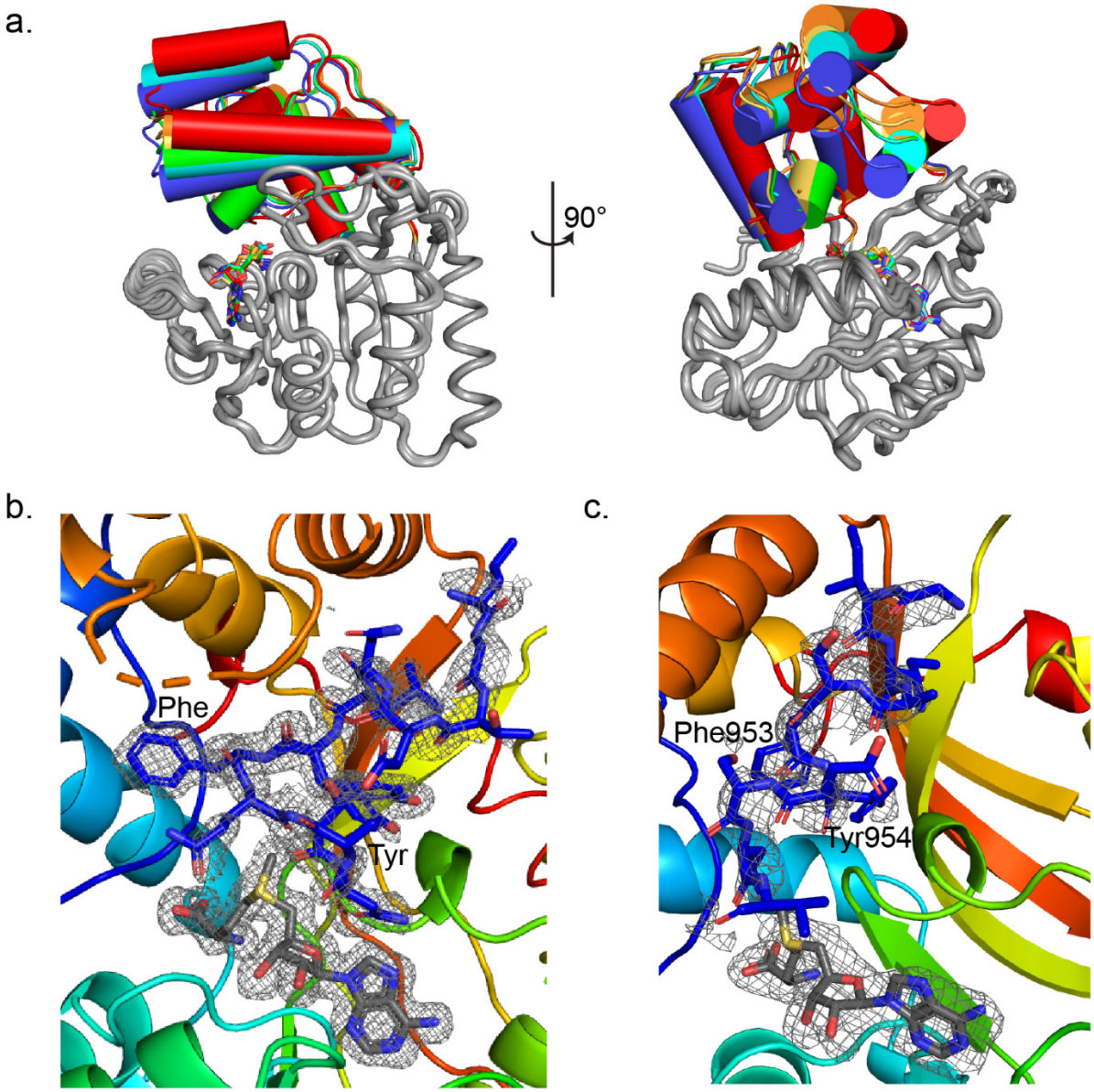

Figure S5 (a) StiD structures aligned at core (123 Cα atoms, gray tube). Regions of the lid differ in position by up to 8 Å. **(b)** StiE *F*o-*F*c omit density for the SAM cofactor and TEV protease recognition sequence (StiE 961-1257, 1.42 Å, 2.5σ contour). Phe and Tyr in the TEV protease recognition sequence are labeled. **(c)** SAM and the partially ordered N-terminal helix (StiE 942-1257, 1.90 Å, *F*o-*F*c omit density contoured at 2.5σ). Conserved Phe953 and Tyr954 in the N-terminal helix are labeled.

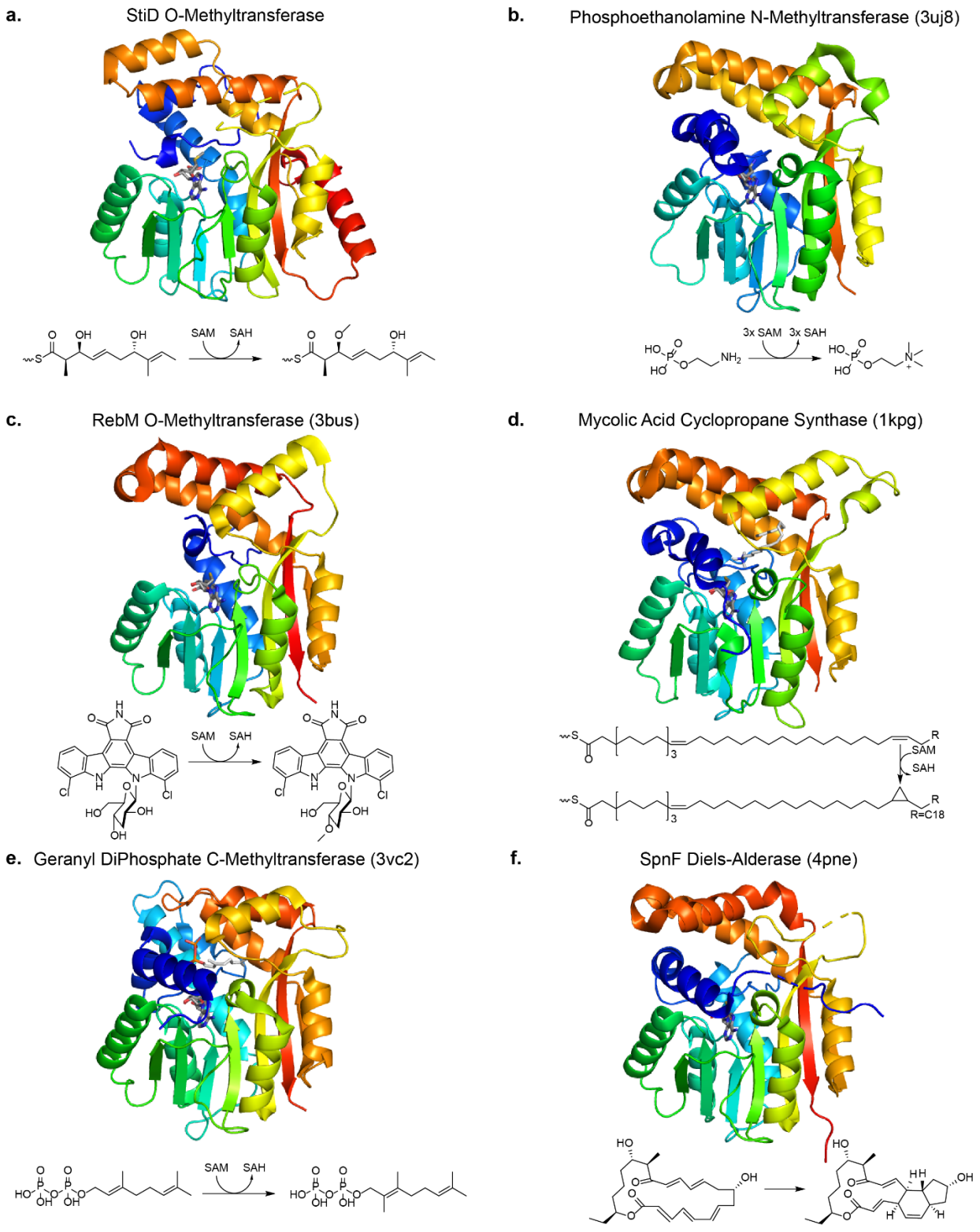

Figure S6. PKS *O*-MT homologs. Structures are colored as a rainbow from N- (dark blue) to C-terminus (red). The reaction catalyzed by each enzyme is shown below the structure. All structures have a lid composed of N-terminal helices (darkest blue) and helices between β-strands 6 and 7 (yellow and orange). SAH or SAM is rendered in stick form with gray C atoms.

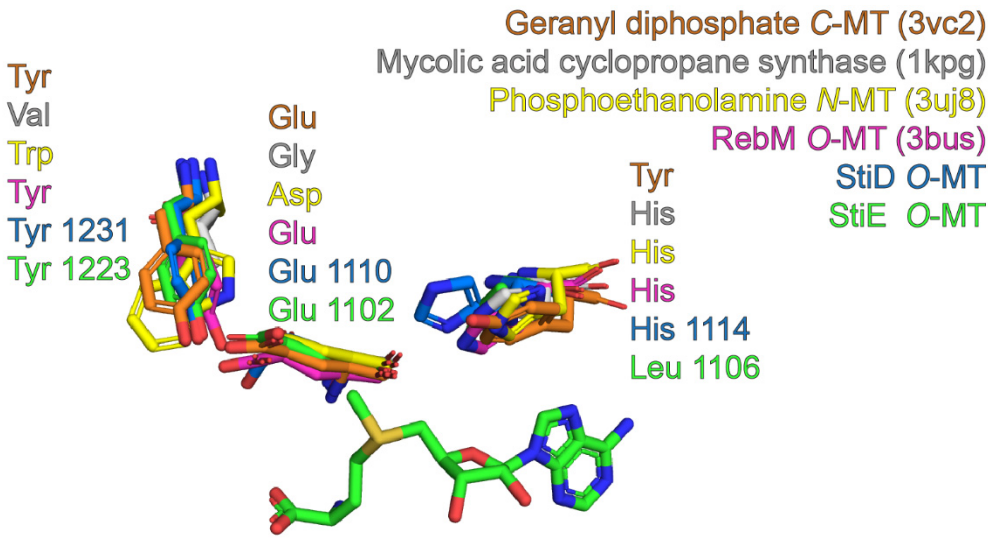

Figure S7. Conservation of key active site residues in structures of StiD and StiE *O*-MTs and homologs.

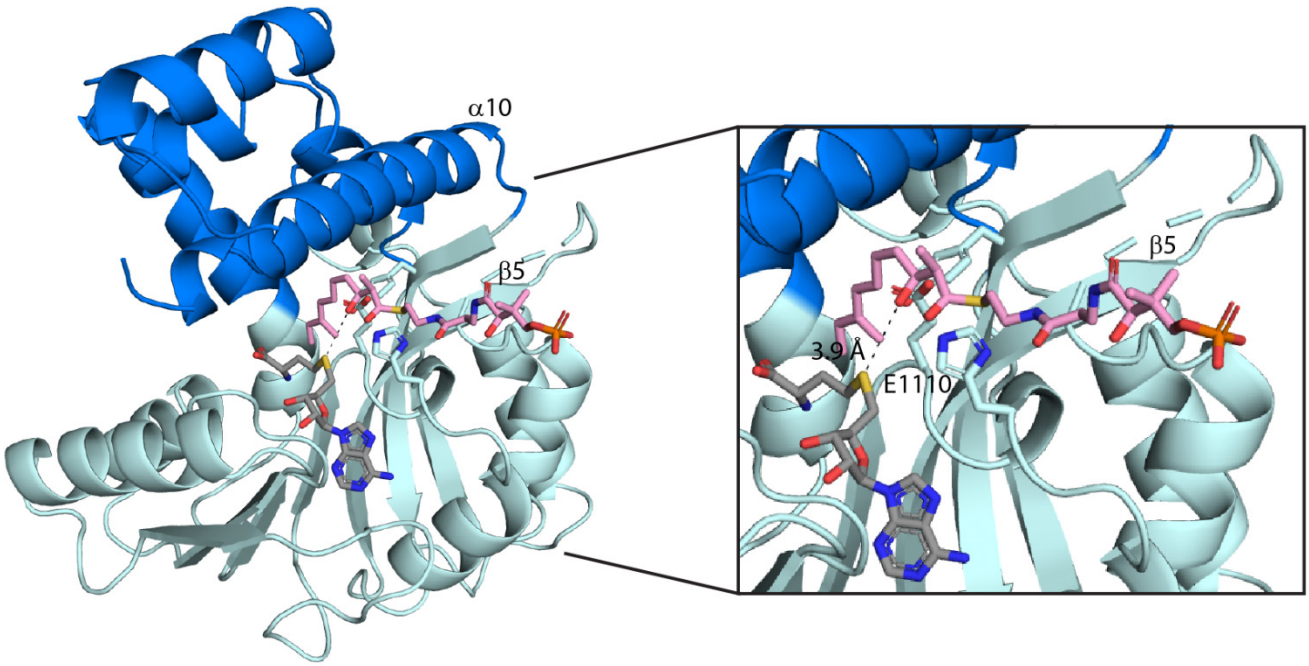

Figure S8. StiD substrate modeling. The full-length StiD substrate (pink sticks with atomic coloring) was modeled with the β-hydroxy oxygen in line with SAH and within hydrogen bonding distance of Glu1110. The ACP may interact with the nine-residue partially ordered loop (StiD 1146-1155). A similar ACP binding site was proposed for the PKS *O*-MT homolog mycolic acid cyclopropane synthase[27].

Table S1. Protein stability of StiD fragments containing the *O*-MT.

	N-950	**N-956**	**N-976**
C-1245	insoluble	insoluble	insoluble
C-1257	insoluble	insoluble	insoluble
C-1266	soluble	soluble	soluble

Table S2. Crystallographic Data

Protein	SeMet StiD 976-1266	StiD 976-1266	StiD 956-1266	StiE 961-1257	StiE 942-1257
Ligand	SAH	SAH	SAH	SAM	SAM
Data Collection					
Space group	*P*1	*P*1	$P4_1$	$P4_32_12$	$P4_32_12$
Unit cell, a,b,c (Å)	38.3, 52.4, 68.7	40.2, 56.2, 72.3	71.1, 71.1, 123.0	90.9, 90.9, 84.9	88.6, 88.5, 86.1
α,β,γ (°)	89.6, 88.3, 81.1	86.3, 84.9, 75.8	90, 90, 90	90, 90, 90	90, 90, 90
X-ray source	APS 23ID-D	APS 23ID-D	APS 23ID-B	APS 23ID-D	APS 23ID-D
Wavelength (Å)	0.979	1.033	1.033	1.033	1.033
d_{min} (Å)	1.96 (2.03-1.96)	1.80 (1.86-1.80)	1.70 (1.76-1.70)	1.42 (1.47-1.42)	1.90 (1.99-1.90)
R-merge	0.066 (0.82)	0.073 (0.74)	0.084 (2.34)	0.064 (1.03)	0.068 (2.28)
Avg I/σ(I)	8.7 (1.1)	9.9 (1.6)	19.8 (1.1)	29.7 (2.7)	21.2 (1.1)
Completeness (%)	96.7 (87.0)	96.7 (94.0)	99.7 (99.9)	99.2 (93.7)	100 (99.7)
Multiplicity	3.5 (2.7)	3.5 (3.5)	13.8 (13.8)	24.3 (19.9)	13.0 (13.1)
Total observations	127,763 (8,823)	193,662 (18,628)	931,727 (92,530)	1,638,916 (124,591)	358,381 (35,303)
Wilson B factor (Å^2)	38.2	27.9	31.3	18.2	41.9
$CC_{1/2}$	0.998 (0.559)	0.997 (0.597)	1.00 (0.442)	1.00 (0.803)	1.00 (0.482)
CC*	1.00 (0.847)	0.999 (0.865)	1.00 (0.783)	1.00 (0.944)	1.00 (0.806)
Refinement					
Data range (Å)	41.3-1.96	38.8-1.80	46.5-1.70	40.6-1.42	44.3-1.90
Reflections	36,668	54,837	67,382	67,269	27,550
R_{work}/R_{free} (%)	17.9/22.7	16.8/19.4	16.8/21.2	16.7/18.5	18.3/22.6
Non-hydrogen atoms (#)	4,629	4,995	4,870	2,768	2,480
protein	4,461	4,628	4,506	2,462	2,311
ligands	52	52	52	27	27
water	116	314	312	315	118
Amino acid residues	554	564	561	279	282
Deviation from ideality					
bond lengths (Å)	0.004	0.007	0.014	0.005	0.007
bond angles (°)	0.99	1.15	1.24	0.88	0.84
Average B-factor (Å^2)	54.6	42.4	48.0	30.5	69.9
protein	54.7	42.1	47.6	29.5	70.3
ligands	54.3	53.9	74.2	18.7	58.1
solvent	51.0	45.7	50.1	39.2	60.9
Ramachandran plot					
favored (%)	97.6	97.7	97.8	97.8	97.1
allowed (%)	2.4	2.3	2	2.2	2.9
outliers (%)	0	0	0.2	0	0
PDB ID	6ECU	6ECV	6ECW	6ECT	6ECX

[1]values in parentheses designate outer shell

Table S3. Primers

StiD 976 F	**TACTTCCAATCCAATGCC**TCAGCCGTGGATGAAAGC
StiD 956 F	**TACTTCCAATCCAATGCC**GAACATCCTGTTGACGGC
StiD 950 F	**TACTTCCAATCCAATGCC**GCGAACGGGCAGGGTAAT
StiD 1245 R	**TTATCCACTTCCAATGCTA**GGTACTACGAACGTGAGAATC
StiD 1257 R	**TTATCCACTTCCAATGCTA**GGCCTCAACCCATTTCTG
StiD 1266 R	**TTATCCACTTCCAATGCTA**CATCAGTTCCCGTGCCGC
StiE 961 F	**TACTTCCAATCCAATGCC**GCGGCGGGGGAAGACG
StiE 951 F	**TACTTCCAATCCAATGCC**GCTTCGTTCTACGATAGCCTG
StiE 942 F	**TACTTCCAATCCAATGCC**GCTTCCGAAGGTACATCAGGC
StiE 1257 R	**TTATCCACTTCCAATGCTA**CGCAAATTCAGCATACGGTGTC
StiD 1794 F	**TACTTCCAATCCAATGCC**GCACTGGCCGCCTTAGG
StiD 1929 R	**TTATCCACTTCCAATGCTA**TTTACGACCTTTATTCAGCGCC
StiE 1789 F	**TACTTCCAATCCAATGCC**GCTCTGCAGTCC
StiE 1927 R	**TTATCCACTTCCAATGCTA**GGCGGTACCTGAG
CurL 951 F	**TACTTCCAATCCAATGCC**TCAAGTTTA
CurL 981 F	**TACTTCCAATCCAATGCC**CAAAAAATGTTGCCTAAGTTGC
CurL 1315 R	**TTATCCACTTCCAATGCTA**AGCTACTTCAGAGTAAGAAGA
StiE Y954F F	AGGCATCATTGCTTCGTTCTTCGATAGCCTGGTG
StiE Y954F R	CACCAGGCTATCGAAGAACGAAGCAATGATGCCT
StiE E1102A F	GATTTAGTGCTCGGATTTGCGGTGGCCGGACTTAT
StiE E1102A R	ATAAGTCCGGCCACCGCAAATCCGAGCACTAAATC
StiE E1102Q F	TGTATGATTTAGTGCTCGGATTTCAGGTGGCCGGAC
StiE E1102Q R	GTCCGGCCACCTGAAATCCGAGCACTAAATCATACA
StiE L1106H F	TGAGGTGGCCGGACATATCCCTGACAAGG
StiE L1106H R	CCTTGTCAGGGATATGTCCGGCCACCTCA
StiE Y1209F F	CAACGTTCCTTTGGCAGCTTTGAGAATGTGTACAAAG
StiE Y1209F R	CTTTGTACACATTCTCAAAGCTGCCAAAGGAACGTTG
StiE Y1223F F	CGGGGGCCTGATCTCCTTTGTACTGTTTCATG
StiE Y1223F R	CATGAAACAGTACAAAGGAGATCAGGCCCCCG
CurL E1161A F	CAACCTGGCATTTGGATTTGCAGTAGCTCATCATATTAAGG
CurL E1161A R	CCTTAATATGATGAGCTACTGCAAATCCAAATGCCAGGTTG
CurL E1161Q F	GATAATTACAACCTGGCATTTGGATTTCAGGTAGCTCATCATATTAAGGAT
CurL E1161Q R	ATCCTTAATATGATGAGCTACCTGAAATCCAAATGCCAGGTTGTAATTATC
CurL Y1281F F	TGCTGTTAGTAATACAAAGCTAGCCAATCCTTTGCTCAG
CurL Y1281 R	CTGAGCAAAGGATTGGCTAGCTTTGTATTACTAACAGCA
CurL Y1010F F	ATTTAAAGGTAATGTAGTTTATGACTATTTCAATTCTTTTGCAGAAATTAGTCAAGAAA
CurL Y1010F R	TTTCTTGACTAATTTCTGCAAAAGAATTGAAATAGTCATAAACTACATTACCTTTAAAT
CurL H1165A F	GGCATTTGGATTTGAAGTAGCTCATGCTATTAAGGATAAATCGCTGTTATTT
CurL H1165A R	AAATAACAGCGATTTATCCTTAATAGCATGAGCTACTTCAAATCCAAATGCC
CurL H1165N F	GCATTTGGATTTGAAGTAGCTCATAATATTAAGGATAAATCGCTGTTAT
CurL H1165N R	ATAACAGCGATTTATCCTTAATATTATGAGCTACTTCAAATCCAAATGC
CurL Y1267F F	ATGTTAAGTCAGCTTTTCAATCCTTTAATCAGTTAGGTAAATTACTGAG
CurL Y1267F R	CTCAGTAATTTACCTAACTGATTAAAGGATTGAAAAGCTGACTTAACAT

Bold text indicates handles for ligation-independent cloning into expression vectors.

SUPPLEMENTARY REFERENCES

1. Gaitatzis, N., Silakowski, B., Kunze, B., Nordsiek, G., Blocker, H., Hofle, G., and Muller, R. The biosynthesis of the aromatic myxobacterial electron transport inhibitor stigmatellin is directed by a novel type of modular polyketide synthase, *J Biol Chem 277*, 13082-13090 (2002).
2. Chang, Z., Sitachitta, N., Rossi, J. V., Roberts, M. A., Flatt, P. M., Jia, J., Sherman, D. H., and Gerwick, W. H. Biosynthetic pathway and gene cluster analysis of curacin A, an antitubulin natural product from the tropical marine cyanobacterium *Lyngbya majuscula*, *J Nat Prod 67*, 1356-1367 (2004).
3. Stols, L., Gu, M., Dieckman, L., Raffen, R., Collart, F. R., and Donnelly, M. I. A new vector for high-throughput, ligation-independent cloning encoding a tobacco etch virus protease cleavage site, *Protein Expr Purif 25*, 8-15 (2002).
4. DelProposto, J., Majmudar, C. Y., Smith, J. L., and Brown, W. C. Mocr: a novel fusion tag for enhancing solubility that is compatible with structural biology applications, *Protein Expr Purif 63*, 40-49 (2009).
5. Skiba, M. A., Maloney, F. P., Dan, Q., Fraley, A. E., Aldrich, C. C., Smith, J. L., and Brown, W. C. PKS-NRPS enzymology and structural biology: considerations in protein production, *Methods Enzymol 604*, 45-88 (2018).
6. Whicher, J. R., Smaga, S. S., Hansen, D. A., Brown, W. C., Gerwick, W. H., Sherman, D. H., and Smith, J. L. Cyanobacterial polyketide synthase docking domains: a tool for engineering natural product biosynthesis, *Chem Biol 20*, 1340-1351 (2013).
7. Sánchez, C., Du, L., Edwards, D. J., Toney, M. D., and Shen, B. Cloning and characterization of a phosphopantetheinyl transferase from *Streptomyces verticillus* ATCC15003, the producer of the hybrid peptide-polyketide antitumor drug bleomycin, *Chem Biol 8*, 725-738 (2001).
8. Evans, D. A., Bartroli, J., and Shih, T. L. Enantioselective aldol condensations. 2. erythro-selective chiral aldol condensations via boron enolates., *Journal of the American Chemical Society 103*, 2127-2129 (1981).
9. Fiers, W. D., Dodge, G. J., Sherman, D. H., Smith, J. L., and Aldrich, C. C. Vinylogous dehydration by a polyketide dehydratase domain in curacin biosynthesis, *J Am Chem Soc 138*, 16024-16036 (2016).
10. May, A. E., Connell, N. T., Dahlmann, H. A., and Hoye, T. R. A useful modification of the evans magnesium halide-catalyzed anti-aldol reaction: application to enolizable aldehydes, *Synlett 13*, 1984-1986 (2010).
11. Gu, L., Wang, B., Kulkarni, A., Gehret, J. J., Lloyd, K. R., Gerwick, L., Gerwick, W. H., Wipf, P., Hakansson, K., Smith, J. L., and Sherman, D. H. Polyketide decarboxylative chain termination preceded by *O*-sulfonation in curacin a biosynthesis, *J Am Chem Soc 131*, 16033-16035 (2009).
12. McCarthy, J. G., Eisman, E. B., Kulkarni, S., Gerwick, L., Gerwick, W. H., Wipf, P., Sherman, D. H., and Smith, J. L. Structural basis of functional group activation by sulfotransferases in complex metabolic pathways, *ACS Chem Biol 7*, 1994-2003 (2012).
13. Dorrestein, P. C., Bumpus, S. B., Calderone, C. T., Garneau-Tsodikova, S., Aron, Z. D., Straight, P. D., Kolter, R., Walsh, C. T., and Kelleher, N. L. Facile detection of acyl and peptidyl intermediates on thiotemplate carrier domains via phosphopantetheinyl elimination reactions during tandem mass spectrometry, *Biochemistry 45*, 12756-12766 (2006).

14. Meluzzi, D., Zheng, W. H., Hensler, M., Nizet, V., and Dorrestein, P. C. Top-down mass spectrometry on low-resolution instruments: characterization of phosphopantetheinylated carrier domains in polyketide and non-ribosomal biosynthetic pathways, *Bioorg Med Chem Lett 18*, 3107-3111 (2008).
15. Kabsch, W. Xds, *Acta Crystallogr D Biol Crystallogr 66*, 125-132 (2010).
16. Zwart, P. H., Afonine, P. V., Grosse-Kunstleve, R. W., Hung, L. W., Ioerger, T. R., McCoy, A. J., McKee, E., Moriarty, N. W., Read, R. J., Sacchettini, J. C., Sauter, N. K., Storoni, L. C., Terwilliger, T. C., and Adams, P. D. Automated structure solution with the PHENIX suite, *Methods Mol Biol 426*, 419-435 (2008).
17. Adams, P. D., Afonine, P. V., Bunkoczi, G., Chen, V. B., Davis, I. W., Echols, N., Headd, J. J., Hung, L. W., Kapral, G. J., Grosse-Kunstleve, R. W., McCoy, A. J., Moriarty, N. W., Oeffner, R., Read, R. J., Richardson, D. C., Richardson, J. S., Terwilliger, T. C., and Zwart, P. H. PHENIX: a comprehensive Python-based system for macromolecular structure solution, *Acta Crystallogr D Biol Crystallogr 66*, 213-221 (2010).
18. Terwilliger, T. C., Grosse-Kunstleve, R. W., Afonine, P. V., Moriarty, N. W., Zwart, P. H., Hung, L. W., Read, R. J., and Adams, P. D. Iterative model building, structure refinement and density modification with the PHENIX AutoBuild wizard, *Acta Crystallogr D Biol Crystallogr 64*, 61-69 (2008).
19. McCoy, A. J., Grosse-Kunstleve, R. W., Adams, P. D., Winn, M. D., Storoni, L. C., and Read, R. J. Phaser crystallographic software, *J Appl Crystallogr 40*, 658-674 (2007).
20. Emsley, P., and Cowtan, K. Coot: model-building tools for molecular graphics, *Acta Crystallogr D Biol Crystallogr 60*, 2126-2132 (2004).
21. Afonine, P. V., Grosse-Kunstleve, R. W., Echols, N., Headd, J. J., Moriarty, N. W., Mustyakimov, M., Terwilliger, T. C., Urzhumtsev, A., Zwart, P. H., and Adams, P. D. Towards automated crystallographic structure refinement with phenix.refine, *Acta Crystallogr D Biol Crystallogr 68*, 352-367 (2012).
22. Chen, V. B., Arendall, W. B., 3rd, Headd, J. J., Keedy, D. A., Immormino, R. M., Kapral, G. J., Murray, L. W., Richardson, J. S., and Richardson, D. C. MolProbity: all-atom structure validation for macromolecular crystallography, *Acta Crystallogr D Biol Crystallogr 66*, 12-21 (2010).
23. Holm, L., and Rosenstrom, P. Dali server: conservation mapping in 3D, *Nucleic Acids Res 38*, W545-549 (2010).
24. Larkin, M. A., Blackshields, G., Brown, N. P., Chenna, R., McGettigan, P. A., McWilliam, H., Valentin, F., Wallace, I. M., Wilm, A., Lopez, R., Thompson, J. D., Gibson, T. J., and Higgins, D. G. Clustal W and Clustal X version 2.0, *Bioinformatics 23*, 2947-2948 (2007).
25. Waterhouse, A. M., Procter, J. B., Martin, D. M., Clamp, M., and Barton, G. J. Jalview Version 2--a multiple sequence alignment editor and analysis workbench, *Bioinformatics 25*, 1189-1191 (2009).
26. Schrodinger, LLC. (2015) The PyMOL Molecular Graphics System, Version 1.8.
27. Huang, C. C., Smith, C. V., Glickman, M. S., Jacobs, W. R., Jr., and Sacchettini, J. C. Crystal structures of mycolic acid cyclopropane synthases from *Mycobacterium tuberculosis*, *J Biol Chem 277*, 11559-11569 (2002).